Membrane Fusion Promoters and Inhibitors Have Contrasting Effects on Lipid Bilayer Structure and Undulations

Thomas J. McIntosh,* Ketan G. Kulkarni,* and Sidney A. Simon[#§]
Departments of *Cell Biology, [#]Neurobiology, and [§]Anesthesiology, Duke University Medical Center, Durham, North Carolina 27710 USA

ABSTRACT It has been established that the fusion of both biological membranes and phospholipid bilayers can be modulated by altering their lipid composition (Chernomordik et al., 1995. *J. Membr. Biol.* 146:3). In particular, when added exogenously between apposing membranes, monomyristoylphosphatidylcholine (MMPC) inhibits membrane fusion, whereas glycerol monoleate (GMO), oleic acid (OA), and arachidonic acid (AA) promote fusion. This present study uses x-ray diffraction to investigate the effects of MMPC, GMO, OA, and AA on the bending and stability of lipid bilayers when bilayers are forced together with applied osmotic pressure. The addition of 10 and 30 mol% MMPC to egg phosphatidylcholine (EPC) bilayers maintains the bilayer structure, even when the interbilayer fluid spacing is reduced to ~3 Å, and increases the repulsive pressure between bilayers so that the fluid spacing in excess water increases by 5 and 15 Å, respectively. Thus MMPC increases the undulation pressure, implying that the addition of MMPC promotes out-of-plane bending and decreases the adhesion energy between bilayers. In contrast, the addition of GMO has minor effects on the undulation pressure; 10 and 50 mol% GMO increase the fluid spacing of EPC in excess water by 0 and 2 Å, respectively. However, x-ray diffraction indicates that, at small interbilayer separations, GMO, OA, or AA converts the bilayer to a structure containing hexagonally packed scattering units ~50 Å in diameter. Thus GMO, OA, or AA destabilizes bilayer structure as apposing bilayers are brought into contact, which could contribute to their role in promoting membrane fusion.

INTRODUCTION

Membrane fusion is a key event in a variety of important biological processes, including exocytosis, endocytosis, synaptic transmission, fertilization, and viral infection. Each of these fusion events has many stages involving membrane docking and subsequent membrane merger events (Vogel et al., 1993; Weber et al., 1998) and is regulated by a variety of specific membrane proteins (see reviews by Hoekstra, 1990; White, 1993; Sudhof, 1995). It is generally agreed that, independent of the mechanisms that cause membranes to adhere, in all membrane fusion events the final step involves the fusion of the lipid bilayers from apposing membranes. This means that the investigation of lipids under conditions where the interbilayer spacings are small may be relevant to understanding fusion events.

Several investigators have found that the exogenous addition of specific lipids can modulate the fusion between biological membranes or lipid vesicles. In many fusion events, including cell-cell fusion (Gunther-Ausborn and Stegmann, 1997), cell syncytia formation (Vogel et al., 1993; Chernomordik et al., 1995c), cortical granule exocytosis (Vogel et al., 1993), organelle-organelle fusion (Chernomordik et al., 1993), virus-lipid vesicle fusion (Yeagle et al., 1994; Gunther-Ausborn et al., 1995), and vesicle-vesicle fusion (Martin and Ruysschaert, 1995), fusion is reversibly inhibited by the exogenous addition of lysophosphatidylcholine (lysoPC) between apposing membranes. On the other hand, the exogenous addition of glycerol monoleate (GMO), oleic acid (OA), or arachidonic acid (AA) has been shown to promote cell-cell fusion (Hope and Cullis, 1981; Chernomordik et al., 1995a–c).

The fusion inhibition produced by lysoPC has been attributed either to lysoPC's effects on fusion-promoting peptides (Martin et al., 1993; Gunther-Ausborn et al., 1995; Gunther-Ausborn and Stegmann, 1997) or its effect on the lipid structure in the membrane (Chernomordik et al., 1993, 1995b; Vogel et al., 1993; Chernomordik and Zimmerberg, 1995; Martin and Ruysschaert, 1995; Razinkov et al., 1998). The fusion promotion produced by GMO, OA, and AA has been attributed to these molecules' effects on lipid organization (Hope and Cullis, 1981; Tilcock and Fisher, 1982; Chernomordik et al., 1995a,c; Chernomordik and Zimmerberg, 1995), although it has been observed that OA interacts with membrane proteins (Hirshic et al., 1993).

In support of the lipid organization models for the effects of lysoPC, GMO, OA, and AA, Chernomordik and colleagues (Chernomordik et al., 1995a–c) note that 1) the membrane merger step of fusion is sensitive to membrane lipid composition but independent of the type of membrane fusion trigger, 2) lysoPC and AA promote opposite spontaneous curvatures in monolayers (Epand, 1985; Epand et al., 1991; Siegel and Epand, 1997), so that high (equimolar) concentrations of GMO convert phospholipid bilayers to a hexagonal (H_{II}) phase (Hope and Cullis, 1981; Tilcock and Fisher, 1982), whereas equimolar quantities of lysoPC convert bilayers to micelles (Van Echteld et al., 1981), and 3) vesicle-planar bilayer fusion is affected in different ways when the same lipids are added to opposite sides of the planar bilayer. Recent studies by Razinkov et al. (1998)

Received for publication 4 May 1998 and in final form 13 January 1999.
Address reprint requests to Dr. Thomas J. McIntosh, Department of Cell Biology, Duke University Medical Center, Box 3011, Durham, NC 27710. Tel.: 919-684-8950; Fax: 919-684-3687; E-mail: tom.mcintosh@cellbio.duke.edu.
© 1999 by the Biophysical Society
0006-3495/99/04/2090/09 $2.00

have also shown that the fusion of cells expressing the hemaglutinin protein of influenza virus with planar lipid bilayers is modified differently by the presence of lipid probes on opposite sides of the bilayer. Chernomordik et al. (1995a,c) argue that lysoPC and GMO may effect fusion by altering the propensity of lipid bilayers to bend by modulating their curvature-elastic energy, and Razinkov et al. (1998) find that the ability of small fusion pores to open is strongly dependent on spontaneous membrane curvature. Specifically, Chernomordik et al. (1995a,c) note that their data are consistent with the hypothesis that membrane fusion proceeds through highly bent lipid intermediates called stalks (Markin et al., 1984; Chernomordik et al., 1987; Kozlov et al., 1989) or through a slightly different type of stalk (as modified by Siegel (1993) and Siegel and Epand (1997)) and transmonolayer contacts (Siegel, 1993; Chernomordik and Zimmerberg, 1995), and Razinkov et al. (1998) argue that in the fusion process the membrane forms a three-dimensional hourglass structure. Chernomordik et al. (1995b) also argue that work arising from this curvature-induced bending energy can be sufficiently large to overcome the repulsive interbilayer hydration pressures (Parsegian et al., 1979; McIntosh and Simon, 1986; Rand and Parsegian, 1989) and push distal monolayers into contact, thus promoting transmonolayer contact formation and subsequent membrane fusion.

Previous work from our laboratory (McIntosh et al., 1995) has shown that the incorporation of large concentrations (50 mol%) of the lysolipid monooleoylphosphatidylcholine (MOPC) into egg phosphatidylcholine (EPC) bilayers decreases the bilayer bending modulus and, as a consequence, significantly increases the repulsive undulation pressure between bilayers. In this paper we consider how the presence of either the fusion inhibitor lysoPC or the fusion promoter GMO modifies the structure and bending (undulatory) properties of EPC membranes. Our studies focus on the relatively small concentrations (~10 mol%) of these lipids that are necessary to inhibit or promote the fusion of biological membranes (Yeagle et al., 1994; Chernomordik et al., 1995b). We use x-ray diffraction of osmotically stressed multilamellar systems to determine the effects of lysoPC and GMO on both the structure and bending properties of phospholipid bilayers. The bending properties are assessed by measuring the long-range component of the repulsive pressure between apposing bilayers, which for neutral phospholipid bilayers is primarily due to bilayer undulations, which depend on the bilayer bending modulus (Evans and Parsegian, 1986; Evans, 1991; McIntosh et al., 1995). We also analyze the structural effects of the fusion promoters OA and AA at small interbilayer separations. In our experiments lysoPC, GMO, OA, or AA is added symmetrically to both monolayers of the bilayer, whereas in most fusion assays these single-chained amphiphiles are added asymmetrically to one side of the membrane. However, as noted recently by Basanez et al. (1998), the asymmetrical requirements for optimal fusion are sometimes difficult to meet experimentally when investigating fusion between biological membranes. Whether an amphiphile acts symmetrically or asymmetrically depends on the rate at which it crosses the bilayer relative to the biological process that is being considered and, in the case of lysoPC, on the amount of lysoPC already present in the membrane.

MATERIALS AND METHODS

Egg phosphatidylcholine (EPC), dioleoylphosphatidylethanolamine (DOPE), and the lysoPC monomyristoylphosphatidylcholine (MMPC) were purchased from Avanti Polar Lipids. Glycerol monoleate (GMO), oleic acid (OA), arachidonic acid (AA), dextran (average molecular weight 580,000), and poly(vinylpyrrolidone) (PVP) (average molecular weight 40,000) were obtained from Sigma Chemical Co.

Two types of lipid systems were examined by x-ray diffraction: unoriented suspensions of multiwalled vesicles and oriented multilayers. The first step in the preparation of both types of samples was to codissolve the appropriate lipid mixture in chloroform. Unoriented liposomes were made by rotary evaporating the chloroform/lipid solution and adding excess (>90% by weight) buffer (100 mM NaCl, 20 mM HEPES, pH 7) containing various concentrations of dextran or PVP. Oriented multilayers were formed by placing a small (5–10 μl) drop of the chloroform/lipid solution on a curved glass substrate and drying under a gentle stream of nitrogen, as described previously (McIntosh et al., 1987, 1989a).

Known osmotic pressures were applied to both of these systems by published procedures (LeNeveu et al., 1977; Parsegian et al., 1979; McIntosh and Simon, 1986; McIntosh et al., 1987). Osmotic stress was applied to the liposomes by incubation in solutions of dextran or PVP. Because these polymers are too large to enter the lipid lattice, they compete for water with the lipid multilayers, thereby applying an osmotic pressure (LeNeveu et al., 1977). Osmotic pressures for dextran and PVP solutions are given by Parsegian et al. (1986). Pressure was applied to the oriented multibilayers by incubating them in constant relative humidity atmospheres maintained with saturated salt solutions, as described by McIntosh et al. (1987, 1989a). The resulting applied pressure (Parsegian et al., 1979) is given by

$$P = -(RT/V_W) \cdot \ln(p/p_o) \quad (1)$$

where R is the molar gas constant, T is the temperature in degrees Kelvin, V_w is the partial molar volume of water, and p/p_o is the ratio of the vapor pressure of the saturated salt solution to the vapor pressure of pure water, which has been determined for a variety of saturated salt solutions (O'Brien, 1948; Weast, 1984).

For both oriented and unoriented specimens, x-ray diffraction patterns were recorded at ambient temperature on stacks of Kodak DEF x-ray film loaded in a flat plate film cassette. The liposome suspensions were sealed in thin-walled x-ray capillary tubes and mounted in a point collimation x-ray camera. The multilayers on the glass substrate were mounted in a controlled humidity chamber on an x-ray camera such that the x-ray beam was oriented at a grazing angle relative to the multilayers. The humidity chamber, which contained a cup of the appropriate saturated salt solution, consisted of a hollow-walled copper cannister with two Mylar windows for passage of the x-ray beam. To speed equilibration, a gentle stream of nitrogen was passed through a flask of the saturated salt solution and then through the chamber. X-ray films were processed by standard techniques and evaluated with a Joyce-Loebl microdensitometer as described previously (McIntosh and Simon, 1986; McIntosh and Holloway, 1987; McIntosh et al., 1987, 1989a). After background subtraction, integrated intensities, $I(h)$, were obtained for each order h by measuring the area under each diffraction peak. For unoriented patterns, the structure amplitude $F(h)$ was set equal to $\{h^2 I(h)\}^{1/2}$ (Blaurock and Worthington, 1966; Herbette et al., 1977). For oriented line-focused patterns, the intensities were corrected by a single factor of h due to the cylindrical curvature of the multilayers (Blaurock and Worthington, 1966; Herbette et al., 1977), so that $F(h) = \{hI(h)\}^{1/2}$.

Electron density profiles, $\rho(x)$, on a relative electron density scale were calculated from

$$\rho(x) = (2/d)\sum \exp\{i\phi(h)\} \cdot F(h) \cdot \cos(2\pi xh/d) \qquad (2)$$

where x is the distance from the center of the bilayer, d is the lamellar repeat period, $\phi(h)$ is the phase angle for order h, and the sum is over h. Phase angles were determined using the sampling theorem (Shannon, 1949) as described in detail previously (McIntosh and Simon, 1986; McIntosh and Holloway, 1987). Electron density profiles presented in this paper are at a resolution of $d/2h_{max} \approx 7$ Å.

RESULTS

For all values of applied osmotic pressure (P), x-ray diffraction patterns from EPC with 0–30 mol% MMPC contained a broad wide-angle band centered at 4.5 Å and several sharp low-angle reflections that indexed as orders of a lamellar repeat period (d). Such patterns are consistent with multilayers of bilayers in the liquid-crystalline (L_α) phase (Tardieu et al., 1973). As shown in Fig. 1, the value of the lamellar repeat period depended on both the concentration of the MMPC in the bilayer and the applied osmotic pressure. In the absence of applied pressure, the repeat period increased monotonically with increasing MMPC concentration from 63 Å for EPC to 77 Å for EPC containing 30 mol% MMPC (shown on the x axis of Fig. 1). No discrete low-angle reflections were recorded from EPC containing 50 mol% MMPC in excess buffer, indicating that this concentration of MMPC produced either micelles or highly disordered multilamellar liposomes. Complete log P versus repeat period curves for EPC containing 0 and 10 mol% MMPC (Fig. 1) showed for both specimens that the repeat period decreased with increasing applied pressure. At high applied pressures (log $P > 7$) the log P versus d curves were similar for the two systems. However, for low applied pressures (log $P < 6$), the addition of MMPC systematically shifted the log P versus d curve, so that at a given low applied pressure the repeat period was increased.

For mixtures of EPC with 10 or 50 mol% GMO in excess buffer or polymer solutions, the x-ray diffraction patterns contained a broad wide-angle band centered at 4.5 Å and two to five low-angle reflections that indexed as orders of a lamellar repeat period. As noted above, such patterns are consistent with multilayers of bilayers in the liquid-crystalline (L_α) phase (Tardieu et al., 1973). The incorporation of GMO into EPC had a relatively small effect on the repeat periods recorded in excess water, as the addition of 10 and 50 mol% GMO increased d by only 0 and 2 Å, respectively (x axis of Fig. 2). Moreover, the addition of 10 or 50 mol% GMO did not significantly modify the pressure-lamellar repeat period curves for log $P < 7.5$ (Fig. 2). However, at log $P > 7.5$ for 50% GMO and log $P > 8.5$ for 10% GMO, the presence of GMO reduced the repeat period (Fig. 2) and, as detailed below, produced intense, sharp reflections located off the lamellar axis, indicating the conversion from a bilayer to a nonlamellar phase.

A Fourier analysis of the lamellar diffraction data was performed to obtain information on the effects of MMPC and GMO on bilayer structure and interbilayer separation. This structural analysis was performed for patterns containing at least four orders of lamellar diffraction. Fig. 3 shows that the structure amplitudes for EPC bilayers with 10 mol% of either MMPC or GMO were very similar to those for EPC bilayers. This indicates that the structure of the bilayer was not markedly changed by these concentrations of MMPC or GMO for the range of applied pressures where

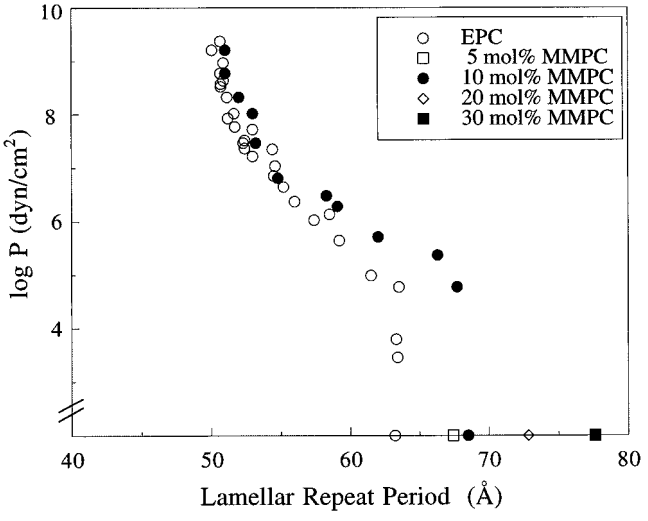

FIGURE 1 The logarithm of applied pressure (log P) plotted versus the lamellar repeat period for EPC bilayers containing 0 and 10 mol% MMPC. Shown on the x axis are the repeat periods in the absence of applied pressure for EPC containing 0, 5, 10, 20, and 30 mol% MMPC. The data for EPC in the absence of MMPC are taken from McIntosh and Simon (1986) and McIntosh et al. (1987).

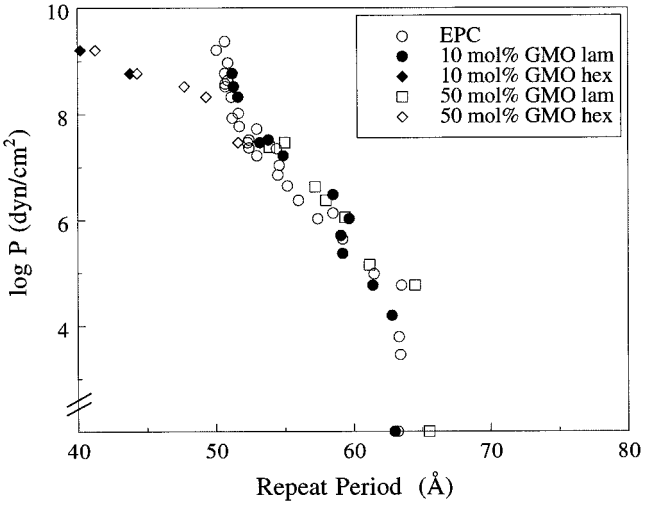

FIGURE 2 The logarithm of applied pressure (log P) plotted versus the repeat period for EPC bilayers containing 0, 10, and 50 mol% GMO. The circles and squares correspond to lamellar repeat periods, and the diamonds correspond to the main repeat from oriented hexagonal diffraction patterns, such as those shown in Fig. 6 *B*. Plotted on the x axis are the lamellar repeat periods in the absence of applied pressure for EPC containing 0, 10, and 50 mol% GMO. The data for EPC are taken from McIntosh and Simon (1986) and McIntosh et al. (1987).

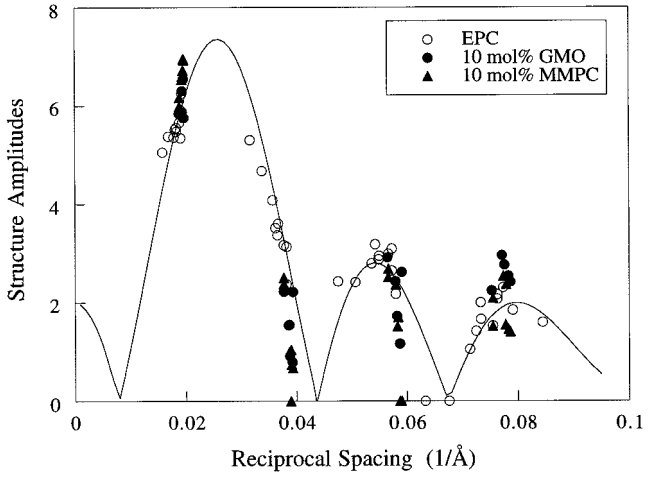

FIGURE 3 Structure amplitudes for the osmotic stress data for EPC and EPC containing 10 mol% MMPC and GMO. The solid line represents the continuous Fourier transform for EPC taken from McIntosh and Simon (1986).

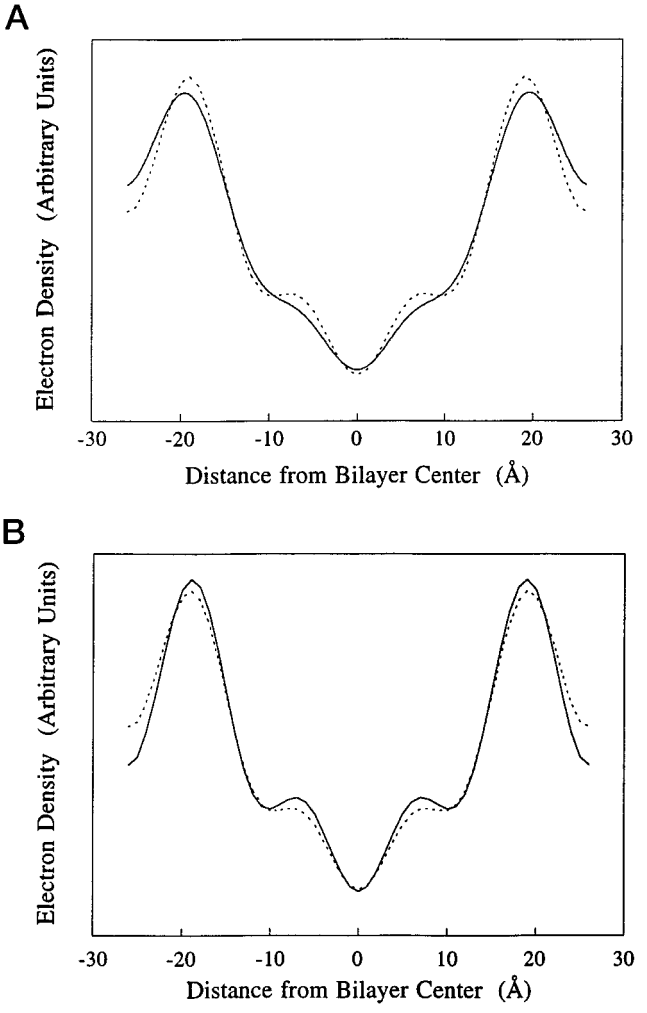

FIGURE 4 Electron density profiles comparing (*A*) EPC (·····) and EPC with 10 mol% MMPC (——) and (*B*) EPC (·····) and EPC with 10 mol% GMO (——). All profiles are from experiments performed at an osmotic pressure of log P = 8.3 (86% relative humidity).

lamellar diffraction was recorded. These structure amplitudes were used to calculate electron density profiles (Eq. 2). Because of the similarity of the structure amplitudes (Fig. 3), we used the same phase angles for EPC:MMPC and EPC:GMO that had previously been used for EPC bilayers (McIntosh and Simon, 1986; McIntosh et al., 1987). Electron density profiles for bilayers at the same applied pressure (log P = 8.3) are shown in Fig. 4 for EPC and EPC with 10 mol% MMPC and GMO. In each profile the geometric center of the bilayer is located at the origin, the low electron density trough in the center of the profile corresponds to the terminal methyl groups at the ends of the hydrocarbon chains, and the high density peaks centered at ±19 Å correspond to the lipid polar headgroups. The intermediate density regions between the terminal methyl troughs and the headgroup peaks correspond to the methylene chain regions, and the medium density regions at the outer edges of each profile correspond to the fluid spacings between apposing bilayers. These profiles show that at this value of applied pressure the incorporation of 10 mol% of either MMPC or GMO had a relatively small effect on bilayer structure. Similar profiles obtained from the lamellar diffraction over the range of applied pressures $7 < \log P < 10$ showed that the separation of high-density headgroup peaks across the bilayer (d_{pp}) was 38.2 ± 0.5 Å (mean ± SD, n = 4 experiments) for EPC with 10 mol% MMPC and 38.1 ± 0.4 Å (n = 5) for EPC with 10 mol% GMO. Over a similar range of applied pressures, d_{pp} = 37.9 ± 0.6 Å (n = 17 experiments) for EPC (McIntosh et al., 1987).

As detailed previously (McIntosh and Simon, 1986; McIntosh et al., 1987, 1989a, 1992), the definition of bilayer thickness is somewhat arbitrary because the bilayer surface is not smooth and water penetrates the headgroup region of the bilayer (Griffith et al., 1974; Worcester and Franks, 1976; Wiener and White, 1991). We operationally define the bilayer width as the total thickness of the bilayer, assuming that the conformation of the phosphorylcholine headgroup in EPC bilayers is the same as it is in single crystals of phosphatidylcholine (Pearson and Pascher, 1979). In that case the high density headgroup peak would be located between the phosphate group and the glycerol backbone. We assume that the phosphorylcholine group is oriented, on average, approximately parallel to the bilayer plane, so that the edge of the bilayer lies ~5 Å outward from the center of the high-density peaks in the electron density profiles (McIntosh and Simon, 1986; McIntosh et al., 1987, 1989a). Therefore, for each osmotic pressure we estimate the bilayer thickness (d_b) from $d_b = d_{pp} + 10$ Å, and the distance between bilayer surfaces (d_f) is calculated from $d_f = d - d_b$.

Using this definition of bilayer thickness, we plot in Fig. 5 the logarithm of applied pressure versus the distance between bilayers for EPC, EPC with 10 mol% MMPC, and EPC with 10 mol% GMO. The data in Fig. 5 indicate that the pressure-d_f relations were very similar for EPC and

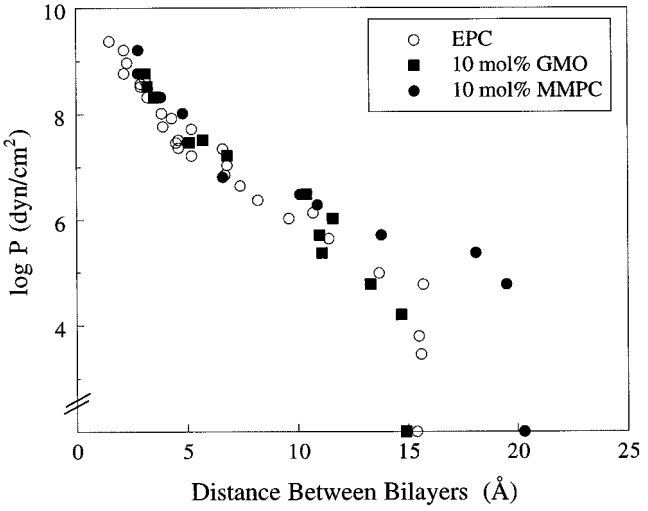

FIGURE 5 The logarithm of applied pressure (log P) plotted versus distance between bilayer surfaces (d_f) for EPC and EPC bilayers containing 10 mol% MMPC and 10 mol% GMO. Shown on the x axis are the values of d_f in the absence of applied pressure.

EPC:GMO bilayers for the entire range of applied pressures. The pressure-d_f relations were also similar for EPC and EPC:MMPC for log $P > 6$. However, at low applied pressures (log $P < 6$), the pressure-d_f curves were shifted to the right by the addition of 10 mol% MMPC. In particular, at zero applied pressure (shown on the x axis), the value of d_f was increased by ~5 Å. These data indicate that the long-range component of the repulsive pressure between EPC bilayers was increased by the addition of 10 mol% MMPC, but not by the addition of 10 mol% GMO.

As noted above, at high applied pressures the incorporation of GMO significantly changed the x-ray diffraction patterns. Fig. 6 compares diffraction patterns recorded from EPC containing 10 mol% GMO recorded at 98% relative humidity (log $P = 7.5$) and 32% relative humidity (log $P = 9.2$). The pattern recorded at log $P = 7.5$ (Fig. 6 *A*) contained several equally spaced equatorial reflections that were oriented perpendicular to the substrate or perpendicular to the surface of the bilayers. The lamellar repeat period was 53 Å. However, at log $P = 9.2$ the pattern (Fig. 6 *B*) was quite different. In addition to multiple orders of an equatorial 40-Å spacing, the patterns contained four additional sharp reflections, each oriented at a 30° angle relative to the substrate, or at a 60° angle relative to the perpendicular from the substrate. The arrow in Fig. 6 *B* points to one of these off-equatorial reflections. Densitometry showed that the relative intensity of each off-axis reflection compared to that of the first equatorial reflection was 0.083 ± 0.009 (mean ± SD, $n = 3$). These additional reflections were at the same 40-Å spacing as the first reflection on the equator of the film. Thus an oriented hexagonal array of reflections was observed, with a primary spacing of 40 Å at log $P = 9.2$. When the applied pressure was reduced to log $P = 7.5$ (by increasing the relative humidity back to 98%), the original 53-Å lamellar repeat period pattern was restored (as in Fig. 6 *A*).

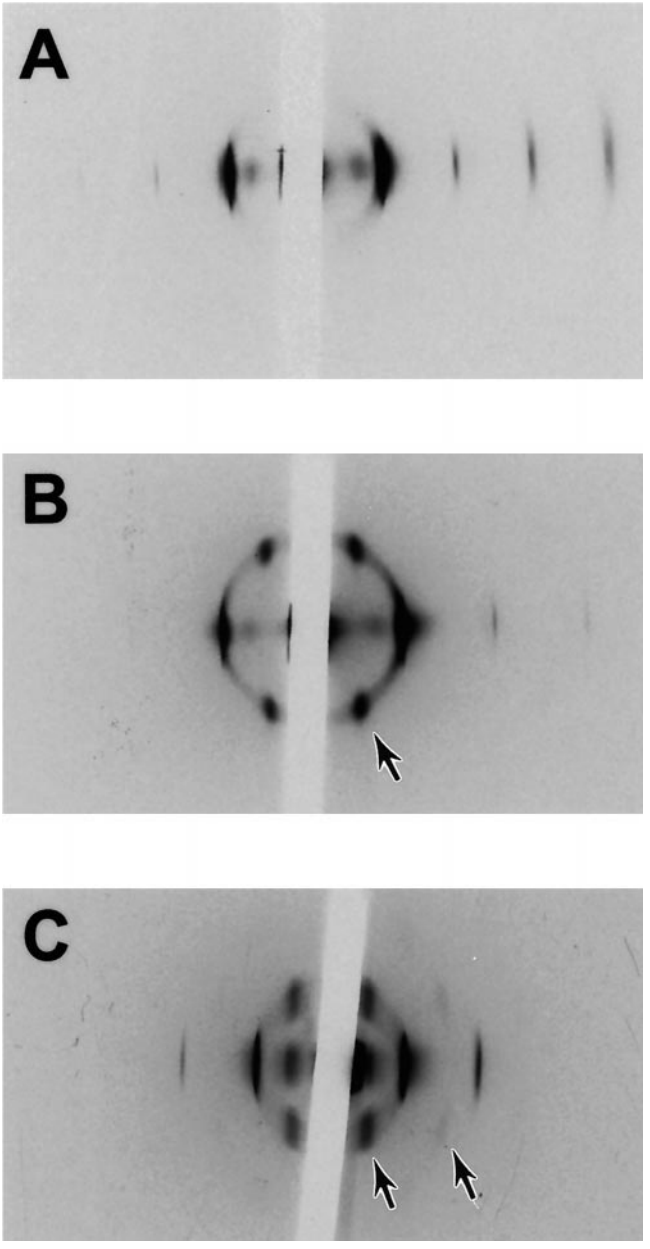

FIGURE 6 X-ray diffraction patterns for (*A*) EPC containing 10 mol% GMO at 98% relative humidity (log $P = 7.5$), (*B*) EPC containing 10 mol% GMO at 32% relative humidity (log $P = 9.2$), and (*C*) EPC containing 30 mol% GMO at 98% relative humidity. The x-ray patterns were recorded from lipid dried on a glass support oriented horizontally. The shadow of the rectangular beam stop is near the center of each pattern. The reflections on the left-hand side of each pattern are lighter than those on the right-hand side because of absorption of x-rays by the glass support. *A* is a typical pattern from oriented bilayers, showing equally spaced lamellar reflections on the equator of the film, oriented perpendicular to the planar bilayers. Patterns *B* and *C* display dark, sharp spots located off the equator of the film that fall on a hexagonal lattice. In *B* the arrow points to the (11) reflection, and in *C* the arrows point to the (11) and (21) reflections.

Oriented hexagonal patterns similar to that shown in Fig. 6 *B* were recorded over a wider range of applied pressures

($7.5 < \log P < 9.5$) for EPC containing 30 and 50 mol% GMO. In some patterns higher orders of a hexagonal lattice could be observed. For example, the pattern in Fig. 6 *C* for EPC containing 30 mol% GMO shows equatorial reflections at 47.6 and 23.8 Å and off-equatorial reflections at 47.6 Å (at a 30° angle relative to the substrate; *left arrow* in Fig. 6 *C*) and at 27.5 Å (at a 60° angle relative to the substrate; *right arrow* in Fig. 6 *C*). These reflections correspond in spacing and orientation to the (10), (20), (11), and (21) orders of a hexagonal lattice with a primary spacing of 47.6 Å. The primary hexagonal spacings decreased with increasing applied pressure; for equimolar EPC:GMO the spacing decreased from 51 Å at $\log P = 7.5$ to 49 Å at $\log P = 8.3$, 44 Å at $\log P = 8.8$, and 41 Å at $\log P = 9.2$ (Fig. 2).

Similar results were obtained for EPC in the presence of 30 mol% oleic acid or arachidonic acid, showing the conversion of a lamellar pattern to the oriented hexagonal pattern at high applied pressures. For EPC with 30 mol% OA, a lamellar phase ($d = 53$ Å) was observed at $\log P = 7.5$, both a lamellar ($d = 51$ Å) and oriented hexagonal lattice ($d = 42$ Å) were recorded on the same film at $\log P = 8.8$, and only a oriented hexagonal lattice ($d = 40$ Å) was observed at $\log P = 9.3$. For EPC with 30% AA, only a lamellar pattern ($d = 53$ Å) was observed at $\log P = 8.3$, both a lamellar ($d = 49$ Å) and oriented hexagonal lattice ($d = 42$ Å) were observed at $\log P = 8.8$, and oriented hexagonal lattices with $d = 42$ Å and 40 Å were recorded at $\log P = 9.2$ and $\log P = 9.3$, respectively. (Complete pressure-distance data were not obtained for bilayers containing the negatively charged OA or AA because electrostatic repulsion would swell these vesicles at low applied pressures.)

For comparison, diffraction patterns were also recorded from oriented specimens of dioleoylphosphatidylethanolamine (DOPE), a lipid that is known to form a hexagonal (H_{II}) phase in unoriented samples with low water contents (Gawrisch et al., 1992). X-ray patterns from DOPE at $\log P = 9.2$ gave a repeat period of 40 Å (data not shown), the same value as recorded for the H_{II} phase of unoriented DOPE at 22°C with two water molecules per lipid molecule (Gawrisch et al., 1992). The first order of this repeating unit was arced. Within this arc most of the intensity was located along the lamellar axis (perpendicular to the plane of the glass substrate), with weak, broad maxima located at angles of 60° relative to the lamellar axis. These off-axis maxima were significantly less intense than the sharp off-axis reflections observed in the patterns shown in Fig. 6, *B* and *C*. Densitometry showed that the relative intensity of each off-axis reflection compared to the first equatorial reflection was 0.030 ± 0.002 (mean ± SD, $n = 3$), or ~36% as intense as the off-axis reflections observed in the hexagonal lattices for EPC with 10 mol% GMO (Fig. 6 *B*).

Experiments were also performed with EPC containing both MMPC and GMO. A sample containing 60% EPC, 20% MMPC, and 20% GMO gave lamellar diffraction patterns over the entire range of applied pressures, with a lamellar repeat period of 68.5 Å at full hydration and a repeat period of 48.4 Å at 32% relative humidity ($\log P = 9.21$). No off-equatorial reflections were observed from oriented specimens at 32% relative humidity with this lipid mixture.

DISCUSSION

The data presented here indicate that at relatively low (10 mol%) concentrations in phosphatidylcholine bilayers, the fusion promoter GMO and the fusion inhibitor MMPC have different effects on bilayer structure, bilayer undulations, and the intermembrane repulsive pressure. The x-ray data also show that at small interbilayer separations the fusion promoters OA and AA produce structural modifications similar to those observed with GMO.

Effects on bilayer structure

The similarity of the electron density profiles (Fig. 4) indicates that the incorporation of 10 mol% of either GMO or MMPC has relatively little effect on the structure of EPC bilayers for applied pressures up to 5.8×10^8 dyn/cm^2 ($\log P = 8.8$). However, at high applied pressures, corresponding to small interbilayer separations ($d_f < 5$ Å; Fig. 5), x-ray patterns such as those in Fig. 6 show that GMO (as well as OA or AA) causes a major rearrangement of the lipid structure. The diffraction patterns in Fig. 6, *B* and *C*, display sharp reflections that index on a hexagonal lattice. For EPC containing 50 mol% GMO, the primary hexagonal spacing decreases systematically from 51 Å to 41 Å with increasing applied pressure. To the best of our knowledge, these are the first patterns from phospholipid specimens to show oriented hexagonal lattices with spacings comparable to the thickness of a lipid bilayer. However, similar diffraction patterns have been obtained with oriented samples of the nonionic detergent hexaethylene glycol mono-*n*-dodecyl ether ($C_{12}EO_6$) (Rançon and Charvolin, 1988b; Clerc et al., 1991). We now consider the structure of this nonlamellar phase observed for EPC:GMO, EPC:OA, and EPC:AA at high applied pressures.

A likely explanation of the hexagonal patterns observed in Fig. 6, *B* and *C*, is the presence of the lipid hexagonal phase (H_{II}) for EPC:GMO at low water contents. Similar patterns from the detergent $C_{12}EO_6$ were interpreted in terms of the hexagonally packed cylinders of a hexagonal phase (Rançon and Charvolin, 1988a,b; Clerc et al., 1991). The patterns recorded from EPC:GMO at low water contents (Fig. 6, *B* and *C*) are similar to those that we recorded from the H_{II} phase of DOPE, except that the off-equatorial intensities were more intense for EPC:GMO than for DOPE. We can think of two possible explanations for this observed difference in intensity distribution. First, there might be a different orientation of the DOPE and EPC:GMO lipid tubes on the glass support. If a larger fraction of the lipid tubes were parallel to the x-ray beam in EPC:GMO than in

DOPE, more of the scattered intensity would be located off the equatorial axis. However, it is not apparent why the lipid tubes of EPC:GMO should have such a preferential orientation on the glass substrate. A second possibility is that there might be a structural difference between the DOPE H_{II} phase and the hexagonal structure of EPC:GMO. For example, the average length of the lipid tubes might be different in the EPC:GMO structure. We note that if the tubes were extremely short they would resemble putative fusion intermediates such as "stalks" (Markin et al., 1984; Kozlov et al., 1989; Siegel, 1993) or "transmonolayer contacts" (Siegel, 1993; Siegel and Epand, 1997).

The observation that the hexagonal pattern (Fig. 6 *B*) observed at low humidities converts back to a typical lamellar (bilayer) phase (Fig. 6 *A*) at high humidities indicates that the hexagonal structure is a stable phase at high applied pressures. Thus the presence of GMO or OA or AA and a small (<5 Å) interlayer spacing is necessary to form this hexagonal lattice structure.

Effects on interbilayer repulsive pressure

For fluid spacings greater than 10 Å, the addition of 10 mol% MMPC has a larger effect on the pressure-distance relationship (Fig. 5) than does the addition of 10 mol% GMO. That is, the addition of 10 mol% MMPC shifts the log P versus d_f curve to the right by as much as 5 Å at low applied pressures. This implies that MMPC increases the magnitude of the total repulsive pressure between bilayers, particularly the long-range component of the pressure thought to be primarily due to thermally induced bilayer undulations (Harbich and Helfrich, 1984; Evans and Parsegian, 1986; Evans, 1991). Previously we (McIntosh et al., 1995) have shown that large concentrations of lysoPC (MOPC) decrease the bilayer bending modulus, thereby increasing the repulsive undulation pressure between bilayers. The data shown in Fig. 5 indicate that the relatively small concentrations (10 mol%) of MMPC that inhibit membrane fusion when added to contact monolayers (Chernomordik et al., 1995b) also increase the total repulsive pressure, most likely by increasing the undulation pressure. On the other hand, 10 mol% GMO does not markedly increase the total repulsive pressure (Fig. 5). Therefore we predict that 10 mol% GMO would have a relatively small effect on the bilayer bending modulus. It is not clear why MMPC and GMO would have different effects on the EPC bilayer bending modulus. One possibility is that MMPC and GMO could have different effects on the configurational entropy of the lipid acyl chains. Another possibility is that because MMPC has a higher critical micelle concentration ($4.3–7.0 \times 10^{-5}$ mol/L; Marsh, 1990) than GMO (4.6×10^{-6} mol/L; Reinhardt and Wachs, 1968), it would have a greater tendency to leave the bilayer and thus decrease the area compressibility modulus (Evans et al., 1995), which is proportional to the bilayer bending modulus.

Relevance to membrane fusion

We have found that the addition of GMO to EPC bilayers does not significantly increase the repulsive pressure between bilayers (Fig. 5), but the fusion promoters GMO, OA, and AA all have a marked effect on the bilayer structure when apposing bilayers are brought close together (interbilayer separations of less than 5 Å). The x-ray evidence indicates that, even when added to both sides of the lipid bilayer, GMO, OA, or AA converts closely apposed bilayers into hexagonal structures containing scattering units ~50 Å in diameter. This destabilization of the bilayer by GMO, OA, or AA could tend to promote membrane fusion.

On the other hand, the symmetrical addition of the fusion inhibitor MMPC has little effect on bilayer structure, even when apposing bilayers are brought close together. Moreover, our experiments with oriented 6:2:2 mixtures of EPC:GMO:MMPC show that MMPC prevents the formation of the hexagonal structure promoted by GMO at low interbilayer spacings. Thus one role of MMPC as a fusion inhibitor might be to increase the energy required for the formation of nonbilayer phases. In contrast to GMO, at low applied pressures MMPC does increase the undulation pressure between bilayers and consequently increases the interbilayer fluid spacing (Fig. 5). This increased repulsion would act to keep apposing bilayers apart, and this increased separation would tend to inhibit fusion. We emphasize that this effect on undulation pressure would only be observed in bilayers with little or no tension (such as unstressed large unilamellar vesicles), and it is unlikely that synaptic vesicles or plasma membranes would be in a stress-free or zero-tension state. Thus the effects of MMPC on the undulation pressure are likely to be small in biological membranes. Nevertheless, our results do show that small concentrations (10 mol%) of MMPC change the bending properties of bilayers in a way that is different from the effect of GMO. Therefore, our results are consistent with the conclusions of Chernomordik and Zimmerberg (1995) regarding the chemically induced bending produced by asymmetrically added lysophospholipids that facilitate fusion when added to contacting monolayers and inhibit fusion when added to distal monolayers.

We thank Drs. Mike Reedy, David Richardson, and Lorena Beese for helpful suggestions concerning the interpretation of the x-ray patterns and Ms. Jennifer Kolodziej for help with the GMO experiments.

This work was supported by grant GM27278 from the National Institutes of Health.

REFERENCES

Basanez, G., F. M. Goni, and A. Alonso. 1998. Effect of single chain lipids on phospholipase C-promoted vescile fusion, a test for the stalk hypothesis of membrane fusion. *Biochemistry.* 37:3901–3908.

Blaurock, A. E., and C. R. Worthington. 1966. Treatment of low angle x-ray data from planar and concentric multilayered structures. *Biophys. J.* 6:305–312.

Chernomordik, L. V., A. Chanturiya, J. Green, and J. Zimmerberg. 1995a. The hemifusion intermediate and its conversion to complete fusion: regulation by membrane composition. *Biophys. J.* 69:922–929.

Chernomordik, L. V., M. M. Kozlov, and J. Zimmerberg. 1995b. Lipids in biological membrane fusion. *J. Membr. Biol.* 146:3.

Chernomordik, L. V., E. A. Leikina, M.-S. Cho, and J. Zimmerberg. 1995c. Control of baculovirus gp64-induced synctium formation by membrane lipid composition. *J. Virol.* 69:3049–3058.

Chernomordik, L. V., G. B. Melikyan, and Y. A. Chimadzhev. 1987. Biomembrane fusion: a new concept derived from model studies using two interacting planar lipid bilayers. *Biochim. Biophys. Acta.* 906: 309–352.

Chernomordik, L. V., S. S. Vogel, A. Sokoloff, H. O. Onaran, E. A. Leikina, and J. Zimmerberg. 1993. Lysolipids reversibly inhibited Ca^{2+}-, GTP- and pH dependent fusion of biological membranes. *FEBS Lett.* 318:71–76.

Chernomordik, L. V., and J. Zimmerberg. 1995. Bending membranes to the task: structural intermediates in bilayer fusion. *Curr. Opin. Struct. Biol.* 5:541–547.

Clerc, M., A. M. Levelut, and J. F. Sadoc. 1991. Transitions between mesophases involving cubic phases in the surfactant-water systems. Epitaxial relations and their consequences in a geometrical framework. *J. Phys. II France.* 1:1263–1276.

Epand, R. M. 1985. Diacylglycerols, lysolecithin, or hydrocarbons alter the bilayer to hexagonal phase transition temperature of phosphatidylethanolamine. *Biochemistry.* 24:7092–7095.

Epand, R. M., R. F. Epand, N. Ahmed, and R. Chen. 1991. Promotion of hexagonal phase formation and lipid mixing by fatty acids with varying degrees of unsaturation. *Chem. Phys. Lipids.* 57:75–80.

Evans, E. 1991. Entropy-driven tension in vesicle membranes and unbinding of adherent vesicles. *Langmuir.* 7:1900–1908.

Evans, E. A., and V. A. Parsegian. 1986. Thermal-mechanical fluctuations enhance repulsion between bimolecular layers. *Proc. Natl. Acad. Sci. USA.* 83:7132–7136.

Evans, E., W. Rawicz, and A. F. Hofmann. 1995. Lipid bilayer expansion and mechanical disruption in solutions of water-soluble bile acid. *In* Bile Acids in Gastroenterology. A. F. Hofmann, G. Paumgurtner, and A. Stiehls, editors. Kluwer Academic, Boston and Dordrecht. 59–68.

Gawrisch, K., V. A. Parsegian, D. A. Hajduk, M. W. Tate, S. M. Gruner, N. L. Fuller, and R. P. Rand. 1992. Energetics of a hexagonal-lamellar-hexagonal-phase transition sequence in DOPE membranes. *Biochemistry.* 31:2856–2864.

Griffith, O. H., P. J. Dehlinger, and S. P. Van. 1974. Shape of the hydrophobic barrier of phospholipid bilayers: evidence for water penetration in biological membranes. *J. Membr. Biol.* 15:159–192.

Gunther-Ausborn, S., A. Praetor, and T. Stegmann. 1995. Inhibition of influenza-induced membrane fusion by lysophosphatidylcholine. *J. Biol. Chem.* 270:29279–29285.

Gunther-Ausborn, S., and T. Stegmann. 1997. How lysophosphatidylcholine inhibits cell-cell fusion mediated by the envelope glycoprotien of human immunodeficiency virus. *Virology.* 235:201–208.

Harbich, W., and W. Helfrich. 1984. The swelling of egg lecithin in water. *Chem. Phys. Lipids.* 36:39–63.

Herbette, L., J. Marquardt, A. Scarpa, and J. K. Blasie. 1977. A direct analysis of lamellar x-ray diffraction from hydrated oriented multilayers of fully functional sarcoplasmic reticulum. *Biophys. J.* 20:245–272.

Hirshic, K. K., B. N. Minnich, L. K. Moore, and J. M. Burt. 1993. Oleic acid differentially affects gap junction-mediated communication in heart and vascular smooth muscle cells. *Am. J. Physiol.* 265:C1515–C1526.

Hoekstra, D. 1990. Membrane fusion of enveloped viruses: especially a matter of proteins. *J. Bioenerg. Biomembr.* 22:121–155.

Hope, M. J., and P. R. Cullis. 1981. The role of nonbilayer lipid structures in the fusion of human erythrocytes induced by lipid fusogens. *Biochim. Biophys. Acta.* 640:82–90.

Kozlov, M. M., S. L. Leikin, L. V. Chernomordik, V. S. Markin, and Y. A. Chizmadzhev. 1989. Stalk mechanism of vesicle fusion. Intermixing of aqueous contents. *Eur. Biophys. J.* 17:121–129.

LeNeveu, D. M., R. P. Rand, V. A. Parsegian, and D. Gingell. 1977. Measurement and modification of forces between lecithin bilayers. *Biophys. J.* 18:209–230.

Markin, V. S., M. M. Kozlov, and V. L. Borovjagin. 1984. On the theory of membrane fusion. The stalk mechanism. *Gen. Physiol. Biophys.* 5:361–377.

Marsh, D. 1990. CRC Handbook of Lipid Bilayers. CRC Press, Boca Raton, FL.

Martin, I., M. C. Dubois, T. Saermark, R. M. Epand, and J. M. Ruysschaert. 1993. Lysophosphatidylcholine mediates the mode of insertion of the NH_2-terminal SIV fusion peptide into the lipid bilayer. *FEBS Lett.* 333:325–330.

Martin, I., and J. M. Ruysschaert. 1995. Lysophosphatidylcholine inhibits vesicle fusion induced by the NH_2-terminal extremity of SIV/HIV fusogenic proteins. *Biochim. Biophys. Acta.* 1240:95–100.

McIntosh, T. J., S. Advani, R. E. Burton, D. V. Zhelev, D. Needham, and S. A. Simon. 1995. Experimental tests for protrusion and undulation pressures in phospholipid bilayers. *Biochemistry.* 34:8520–8532.

McIntosh, T. J., and P. W. Holloway. 1987. Determination of the depth of bromine atoms in bilayers formed from bromolipid probes. *Biochemistry.* 26:1783–1788.

McIntosh, T. J., A. D. Magid, and S. A. Simon. 1987. Steric repulsion between phosphatidylcholine bilayers. *Biochemistry.* 26:7325–7332.

McIntosh, T. J., A. D. Magid, and S. A. Simon. 1989a. Cholesterol modifies the short-range repulsive interactions between phosphatidylcholine membranes. *Biochemistry.* 28:17–25.

McIntosh, T. J., A. D. Magid, and S. A. Simon. 1989b. Range of the solvation pressure between lipid membranes: dependence on the packing density of solvent molecules. *Biochemistry.* 28:7904–7912.

McIntosh, T. J., and S. A. Simon. 1986. The hydration force and bilayer deformation: a reevaluation. *Biochemistry.* 25:4058–4066.

McIntosh, T. J., S. A. Simon, D. Needham, and C.-h. Huang. 1992. Interbilayer interactions between sphingomyelin and sphingomyelin: cholesterol bilayers. *Biochemistry.* 31:2020–2024.

O'Brien, F. E. M. 1948. The control of humidity by saturated salt solutions. *J. Sci. Instrum.* 25:73–76.

Parsegian, V. A., N. Fuller, and R. P. Rand. 1979. Measured work of deformation and repulsion of lecithin bilayers. *Proc. Natl. Acad. Sci. USA.* 76:2750–2754.

Parsegian, V. A., R. P. Rand, N. L. Fuller, and R. C. Rau. 1986. Osmotic stress for the direct measurement of intermolecular forces. *Methods Enzymol.* 127:400–416.

Pearson, R. H., and I. Pascher. 1979. The molecular structure of lecithin dihydrate. *Nature.* 281:499–501.

Rançon, Y., and J. Charvolin. 1988a. Epitaxial relationships during phase transformations in a lyotropic liquid crystal. *J. Phys. Chem.* 92: 2646–2651.

Rançon, Y. and J. Charvolin. 1988b. Fluctutations and phase transformation in a lyotropic liquid crystal. *J. Phys. Chem.* 92:6339–6344.

Rand, R. P., and V. A. Parsegian. 1989. Hydration forces between phospholipid bilayers. *Biochim. Biophys. Acta.* 988:351–376.

Razinkov, V. I., G. B. Melikyan, R. M. Epand, R. F. Epand, and F. S. Cohen. 1998. Effects of spontaneous curvature on influenza virus-mediated fusion pores. *J. Gen. Physiol.* 112:409–422.

Reinhardt, V. R., and W. Wachs. 1968. Beziehungen zwischen grenzflächenaktiven eigenschaften und polarität bei fettsäuremonoglyceriden. *Tenside.* 5:125–131.

Shannon, C. E. 1949. Communication in the presence of noise. *Proc. Inst. Radio Engineers N.Y.* 37:10–21.

Siegel, D. P. 1993. Energetics of intermediates in membrane fusion: comparison of stalk and inverted micellar intermediate mechanisms. *Biophys. J.* 65:2124–2140.

Siegel, D. P., and R. M. Epand. 1997. The mechanism of lamellar-to-inverted hexagonal phase transitions in phosphatidylethanolamine: implications for membrane fusion mechanisms. *Biophys. J.* 73:3089–3111.

Sudhof, T. C. 1995. The synaptic vesicle cycle: a cascade of protein-protein interactions. *Nature.* 375:645–653.

Tardieu, A., V. Luzzati, and F. C. Reman. 1973. Structure and polymorphism of the hydrocarbon chains of lipids: a study of lecithin-water phases. *J. Mol. Biol.* 75:711–733.

Tilcock, C. P., and D. Fisher. 1982. Interactions of glycerol monooleate and dimethylsulphoxide with phsopholipids. A differential scanning calorimetry and ^{31}P-NMR study. *Biochim. Biophys. Acta.* 685:340–346.

Van Echteld, C. J. A., B. DeKruijff, J. G. Mandersloot, and J. DeGier. 1981. Effects of lysophophatidylcholines on phosphatidylcholine and phosphatidylcholine/cholesterol liposome systems as revealed by ^{31}P-NMR, electron microscopy, and permeability studies. *Biochim. Biophys. Acta.* 649:211–220.

Vogel, S. S., E. A. Leikina, and L. V. Chernomordik. 1993. Lysophosphatidylcholine reversibly arrests exocytosis and viral fusion at a stage between triggering and membrane merger. *J. Biol. Chem.* 268: 25764–25768.

Weast, R. C. 1984. Handbook of Chemistry and Physics. CRC Press, Boca Raton, FL.

Weber, T., B. V. Zemelman, J. A. McNew, B. Westermann, M. Gmachl, F. Parlati, T. H. Soliner, and J. E. Rothman. 1998. SNAREpins: minimal machinery for membrane fusion. *Cell.* 92:759–772.

White, J. M. 1993. Membrane fusion. *Science.* 258:917–924.

Wiener, M. C., and S. H. White. 1991. Fluid bilayer structure determination by the combined use of x-ray and neutron diffraction. II. "Composition-space" refinement method. *Biophys. J.* 59:174–185.

Worcester, D. L., and N. P. Franks. 1976. Structural analysis of hydrated egg lecithin and cholesterol bilayers. II. Neutron diffraction. *J. Mol. Biol.* 100:359–378.

Yeagle, P. L., F. T. Smith, J. E. Young, and T. D. Flanagan. 1994. Inhibition of membrane fusion by lysophosphatidylcholine. *Biochemistry.* 33:1820–1827.